nature photonics

OCTOBER 2012 VOL 6 NO 10
www.nature.com/naturephotonics

X-RAY FELS
Self-seeding success

SPIN-WAVE EMISSION
Directional control by light

SILICON NANOPHOTONICS
Bridging mid-infrared gap

Ultrastable silicon Fabry–Pérot cavity

nature photonics

ARTICLES

PUBLISHED ONLINE: 9 SEPTEMBER 2012 | DOI: 10.1038/NPHOTON.2012.217

A sub-40-mHz-linewidth laser based on a silicon single-crystal optical cavity

T. Kessler[1], C. Hagemann[1], C. Grebing[1], T. Legero[1], U. Sterr[1], F. Riehle[1]*, M. J. Martin[2], L. Chen[2†] and J. Ye[2]*

State-of-the-art laser frequency stabilization by high-finesse optical cavities is limited fundamentally by thermal noise-induced cavity length fluctuations. We present a novel design to reduce this thermal noise limit by an order of magnitude as well as an experimental realization of this new cavity system, demonstrating the most stable oscillator of any kind to date for averaging times of 0.1–10 s. The cavity spacer and the mirror substrates are both constructed from single-crystal silicon and are operated at 124 K, where the silicon thermal expansion coefficient is zero and the mechanical loss is small. The cavity is supported in a vibration-insensitive configuration, which, together with the superior stiffness of the silicon crystal, reduces the vibration-related noise. With rigorous analysis of heterodyne beat signals among three independent stable lasers, the silicon system demonstrates a fractional frequency instability of 1×10^{-16} at short timescales and supports a laser linewidth of <40 mHz at 1.5 μm.

Precision optical interferometers are at the heart of the world's most accurate measuring science, including optical atomic clock work[1–3], gravitational wave detection[4,5], cavity quantum electrodynamics[6], quantum optomechanics[7,8] and precision tests of relativity[9]. These experiments explore the next frontiers of measurement science and open new windows for scientific discoveries. The ultimate limit to the sensitivity and stability of these interferometry devices is now set by the Brownian thermomechanical noise in the interferometer mirrors or spacers[10–12]. This noise leads directly to fluctuations in the optical length of the interferometer, degrading the frequency stability of any laser stabilized to it[13–15] and impeding the achievement of quantum coherence in a macroscopic system. Consequently, attempts have been made—both theorically[12,16] and experimentally[17,18]—to lower this limit, which, at best, is currently given by a fractional instability of $\sim 2 \times 10^{-16}$ for averaging times below 10 s (refs 14,15).

Here, we present an approach capable of reducing this thermal noise limit by at least an order of magnitude. As a result of the fluctuation-dissipation theorem, the thermal noise of an interferometer made of a crystalline material with a high mechanical quality factor Q can be reduced significantly compared with conventional glass materials. Crystalline material can have a superior Young's modulus that effectively suppresses the sensitivity of the cavity length to environmental vibration noise. Furthermore, aging-related frequency drifts, which are commonly encountered in conventional glass materials, can be suppressed in crystalline materials, as demonstrated by cryogenic sapphire optical resonators operated at a temperature of 4.2 K, which have shown a maximum change in frequency of 2.7 kHz over six months[19]. However, in these earlier experiments, the short-term instability was limited to a level of 2.3×10^{-15} for averaging times of 20 s (ref. 20) due to vibrations of the cryostat.

In our study, we selected silicon single crystal as the high-Q material for both the cavity spacer and mirror substrates. In contrast to sapphire, an all-silicon interferometer can be made insensitive to temperature fluctuations as the coefficient of thermal expansion of silicon has a zero crossing near 124 K. In this temperature range, the Q of silicon is orders of magnitude higher than that of conventional cavity glass materials such as ultralow expansion glass (ULE) or fused silica[21]. A similar approach has been used with relatively low-finesse optical Fabry–Pérot interferometers[22] and has recently been proposed for gravitational wave detection[23]. A further issue to be solved is the thermal noise associated with the optical coating, but its contribution can be reduced by using a longer cavity spacer.

After presenting the detailed design of the silicon crystal cavity, we report the frequency stabilization of a laser to a high-finesse silicon interferometer at a wavelength of 1.5 μm, which is in the near-infrared transmission window of the silicon substrate between 1.1 and 6.7 μm. By comparison with two other lasers stabilized to state-of-the-art conventional interferometers, we demonstrate the superior performance of the silicon interferometer by achieving a laser linewidth of <40 mHz and short-term instability at 1×10^{-16}. The corresponding optical coherence length is $>1 \times 10^{9}$ m, on the order of the length of the proposed Laser Interferometer Space Antenna (LISA). Although this performance exceeds that of any oscillator demonstrated to date in the microwave or optical regions, we emphasize that the novel approach comprising the use of a single-crystal silicon cavity instead of more traditional materials such as ULE or sapphire will enable much greater progress in relation to time, frequency and space–time metrology.

Design of the silicon cavity

Monocrystalline silicon has superior mechanical properties[24], including a high elastic modulus (well above that of optical glasses) and large thermal conductivity. This thermal conductivity (500 W m^{-1} K^{-1} at 124 K; ref. 25) is about two orders of magnitude higher than that of glass (1.31 W m^{-1} K^{-1}), which assures an homogeneous temperature and small local heating from any absorbed laser radiation. Silicon is a cubic crystal with its largest Young's modulus along the <111> axis ($E = 187.5$ GPa)[26]; we have chosen this axis to be the optical axis of the cavity. Taking

[1]Physikalisch-Technische Bundesanstalt, Bundesallee 100, 38116 Braunschweig, Germany, [2]JILA, National Institute of Standards and Technology and University of Colorado, Department of Physics, 440 UCB, Boulder, Colorado 80309, USA; [†]Present address: Wuhan Institute of Physics and Mathematics, Chinese Academy of Sciences, Wuhan, 430071, China. *e-mail: fritz.riehle@ptb.de; ye@jila.colorado.edu

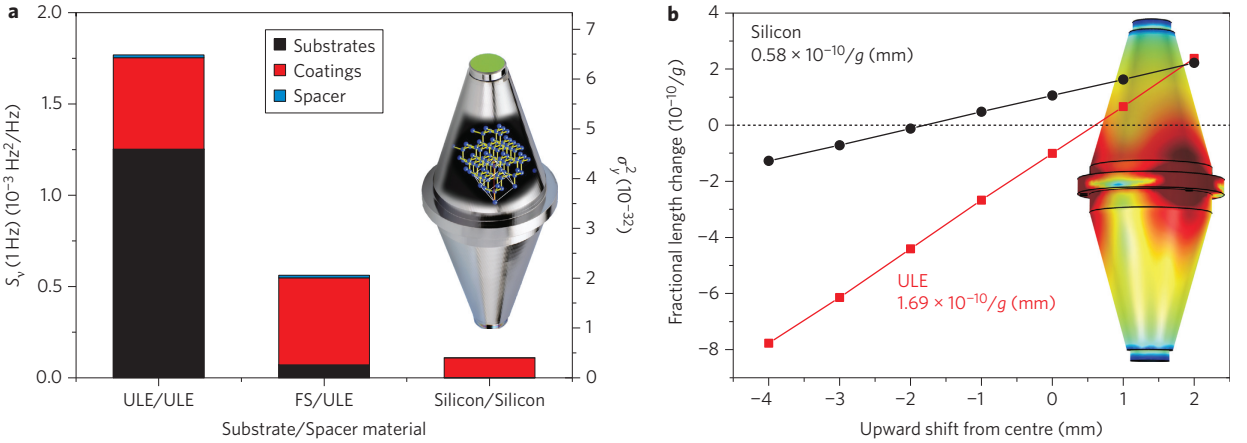

Figure 1 | Performance of a single-crystal silicon Fabry–Pérot interferometer. a, Estimation of frequency noise power spectral density arising from Brownian-motion thermal noise for various mirror substrate and spacer materials at their corresponding zero crossing temperatures. The nominal dimension of the optical cavity has a spacer length of 210 mm, spacer radius of 50 mm, central bore of 5 mm, radii of curvature of 1 m/∞ for the two mirrors. Right axis: corresponding Allan variance for fractional optical frequency instability (Allan variance is the square of Allan deviation presented in subsequent figures). **b**, FEM simulation of the vibration sensitivity of the vertical cavity design as a function of position of the central support ring from the symmetric plane, for ULE and single-crystal silicon as cavity materials. Inset: strain energy distribution for the silicon spacer.

into account the density ρ of silicon (2.33 g cm^{-3}), one obtains a specific stiffness of $E/\rho \approx 80 \times 10^6$ m^2 s^{-2} along this axis, compared to $\sim 30 \times 10^6$ m^2 s^{-2} for ULE.

Figure 1a shows the calculated thermal noise for the silicon cavity at its zero crossing temperature of 124 K, as well as data for room-temperature cavities with ULE spacers and ULE or fused-silica mirror substrates. The frequency noise power spectral density of the silicon cavity-stabilized laser is reduced partially because of the lower temperature. In addition, the high mechanical quality factor of silicon ($Q > 10^7$; ref. 27) directly reduces the noise contribution from the spacer and the mirror substrates. The high Young's modulus of the mirror substrate compared to ULE and fused silica ($E \approx 67.6$ GPa) also further reduces the thermal noise of the coating[28]. Combining these contributions, we estimate that the thermal noise leads to a flicker floor of the fractional optical frequency instability of $\sigma_y = 7 \times 10^{-17}$. In the extremely unlikely scenario where the substrate temperature is set 1 K off the zero crossing point of the thermal expansion, the estimated thermo-optic (coating) and thermo-elastic (substrate) noise is at least two orders of magnitude below this thermal noise.

To reach this record-low level of thermal noise, we must reduce the influence of environmental vibrations on the resonator (length $L = 210$ mm). We minimized the sensitivity of the spacer length to external applied forces by means of finite element modelling (FEM), taking advantage of the full elasticity tensor of silicon. Designs with either a vertical[13,29] or a horizontal optical axis[30,31] have achieved strong suppression of vibrational sensitivity. After extensive FEM simulations, a vertical configuration similar to that of ref. 13 was chosen, as it showed the smallest sensitivity to the details of the mounting (for example, contact area and contact material). We found that $\Delta L/L$ was $<10^{-10}/g$ for a tolerance of the axial position of 0.5 mm ($g = 9.81$ m s^{-2} is the acceleration due to gravity and $\Delta L/L$ is the fractional length change of the cavity). This represents a factor of three improvement over a ULE cavity of the same design.

It is important to note that the anisotropic structure of silicon leads to a dependence of the vibration sensitivity on the location of the support points with respect to the crystal axes. We found that the <110> directions offered the optimal supporting configuration. The three equivalent directions of <110> intersect with our horizontal mounting ring, giving rise to three supporting points that are symmetric by axial rotation through 120°. Horizontal accelerations bend the cavity, leading to a tilt of the mirrors of 65 nrad/g with respect to the symmetry axis, compared to 180 nrad/g for ULE. Finally, for a 10% asymmetry in the elasticity between the mounting points we found an on-axis fractional length change of $2 \times 10^{-11}/g$ ($5 \times 10^{-11}/g$ for ULE). These results clearly illustrate the superior elastic properties of silicon compared to low-expansion glass.

The raw material was a low-impurity silicon rod with a resistivity of $\sim$30 kΩ cm and a diameter of 100 mm. It was oriented by X-ray diffraction to define the optical axis to within 10^{-3} radians. The crystal was machined to a tapered cylindrical shape with a mounting ring and the surface was etched to reduce stress induced by the machining process[13]. The silicon mirror substrates were machined from the same oriented material and, after being superpolished and coated with high-reflectivity low-loss optical thin films, they were optically contacted to the spacer. We aligned the substrates and spacer crystal in the same crystallographic orientation as to best maintain the single-crystal property of the entire cavity. We are able to obtain a finesse of 240,000 for the TEM01 mode of the cavity. A finesse of just 80,000 was achieved for the TEM00 mode, most probably because of local contamination of the coating. Consequently, for all the results discussed in this work, the TEM01 mode was used for laser stabilization.

Cryostat design and performance

A fractional frequency instability at the level of 1×10^{-16} also places a stringent requirement on cavity temperature stabilization. Thermal fluctuations are suppressed to first order by operating the cavity at a zero crossing point of its thermal expansion ($\sim$124 K for silicon[33]). A major challenge for optical cavities operated at cryogenic temperatures is the reduction of vibrations induced by the cooling mechanism. This challenge was overcome in part by a novel and simple cryostat design based on nitrogen gas as the coolant. A sketch of the set-up is shown in Fig. 2. The vacuum chamber was placed on an actively controlled vibration isolation table and evacuated to a residual pressure of 1×10^{-8} mbar. The cavity was surrounded by two massive, cylindrical, gold-plated copper shields and supported by a tripod machined from Teflon. Cooling of the outer shield was accomplished by evaporating liquid nitrogen from a Dewar using a heating resistor. The nitrogen gas flowed through superinsulated vacuum tubes to the outer heat shield and, by regulating its flow, the shield temperature

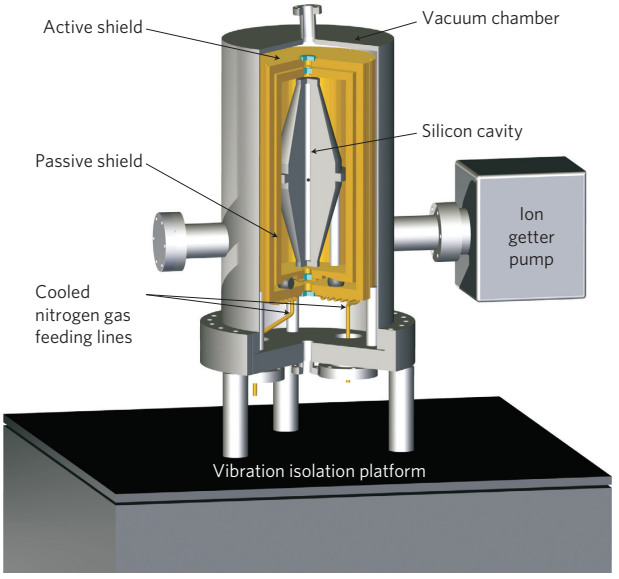

Figure 2 | Schematic of the vibration-reduced, nitrogen-gas-based cryostat, including the vacuum chamber and two heat shields centred around the silicon single-crystal cavity. The thermal time constant of the system is 10 days.

was stabilized to maximum deviations of ~1 mK from the setpoint. An additional thermally isolated passive heat shield was used to suppress radiative heat transfer from the outer shield to the silicon cavity. We measured a thermal time constant of 10 days, dominated by the heat capacity of the inner shield. During continuous operation, the cryostat exhibited acceleration noise of a few 0.1 μg $Hz^{-1/2}$ in the frequency range 1–100 Hz.

The cavity length was probed by a commercial erbium-doped fibre laser source. Locking to the cavity resonance was realized by means of the Pound–Drever–Hall (PDH) scheme[32]. Phase modulation of the laser was achieved using an all-fibre waveguide electro-optical modulator with an active suppression of the residual amplitude modulation (RAM) (see Methods). Feedback was applied to a fibre-coupled acousto-optical modulator with a locking bandwidth of ~200 kHz to keep the laser tightly locked to the cavity resonance.

The coefficient of thermal expansion, α, of the silicon cavity was measured in a region close to its predicted zero crossing at 124 K by monitoring the frequency of the laser locked to the cavity as a function of the cavity temperature measured on its surface (using a PT-100 sensor). The laser frequency was measured in comparison to a reference laser system stabilized at room temperature. The minimum cavity length was found at a temperature of 124.2(1) K, with the dominating uncertainty arising from sensor calibration. We determined a zero crossing sensitivity of $d\alpha/dT = 1.71(1) \times 10^{-8}\,K^{-2}$. These results are consistent with the values given in ref. 33 and are to be compared to a value of $d\alpha/dT = 1.8 \times 10^{-9}\,K^{-2}$ obtained for ULE.

To determine the sensitivity of the cavity length to vibrations in the horizontal and vertical directions (k_x, k_y and k_z, respectively), we analysed the frequency response of the stabilized laser system to applied excitations. We measured accelerations in all three axes while simultaneously recording the frequency of the silicon cavity-stabilized laser system with a second reference laser system. As we observed a non-negligible coupling of the movement from the excited to the non-excited directions, we had to take into account amplitude and phase relations of all acceleration components in the full calculation[30]. For the horizontal directions, fractional vibration sensitivities of $k_x = 6.7(3) \times 10^{-11}/g$ and $k_y = 8.4(4) \times 10^{-11}/g$ were determined. The vertical sensitivity was determined to be $k_z = 5.5(3) \times 10^{-11}/g$. These values readily enable an instability of $\sigma_y < 10^{-16}$ in 1 s and are to be compared to the values of $2.45(3)/0.21(4)/0.01(1) \times 10^{-11}/g$ reported for the vibration sensitivities of a state-of-the-art ULE cavity in the axial and two transverse directions[34].

Reference laser systems

To determine the performance of the silicon cavity-stabilized laser, we used two of the best-performing conventional ULE-based optical cavity-stabilized lasers from JILA and PTB. Using heterodyne beats between these three independently stabilized lasers, we performed a three-cornered hat comparison[35] at 1.5 μm.

The first reference laser (REF. 1) built at PTB was designed as a compact cavity-stabilized system. A distributed feedback fibre laser was stabilized to a horizontally mounted reference cavity made of ULE. The cavity is 10 cm long and has a finesse of 316,000. The thermal noise of the cavity is expected to limit the Allan deviation at a flicker floor of $\sigma_y(\tau) \approx 6 \times 10^{-16}$.

The second reference system (REF. 2), constructed at JILA and set up at PTB, uses another erbium-doped fibre laser frequency stabilized to a ULE cavity. The mirror substrate material is fused silica, which lowers the magnitude of the thermally driven mirror fluctuations in comparison to a system employing ULE mirror substrates. Furthermore, the cavity spacer length of 25 cm reduces the fractional impact of these same fluctuations on the frequency stability of the cavity-stabilized laser, resulting in an expected thermal noise-limited flicker floor of 2×10^{-16}. The cavity finesse is 80,000, which led to a comparatively increased sensitivity to time-dependent RAM caused by parasitic effects, making active RAM stabilization mandatory (see Methods).

To make simultaneous comparisons of the three systems, the frequency-stable light of each of the three laser systems was transferred by single-mode optical fibres to a centrally located beat detection unit. A fibre noise cancellation system[36] for each optical fibre path reduced the fibre noise to a level of instability below 10^{-16} at 1 s. At the central detection unit the light of all three lasers was superimposed on 50/50 fibre-splitters. An InGaAs photodiode at the output of the last fibre-splitter detected the three beat signals. The laser beat signals were tracked by phase-locked-loop-based filters and subsequently recorded by a dead-time free counter (K + K Messtechnik, model FXE) in phase averaging mode, which corresponds to an overlapping Λ-mode counting scheme as required for the measurement of the modified Allan deviation[37,38]. This measure for the stability of the oscillators was chosen to obtain the highest possible sensitivity at averaging times greater than 100 ms, where we expect to reach the thermal noise floor.

Laser frequency stability

To characterize the performance of all three lasers, a 24 h record of the beat signal was taken with a counter gate time of 100 ms.

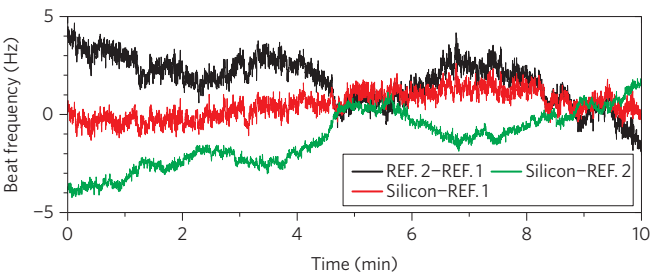

Figure 3 | Traces of the three beats involved in the three-cornered hat comparison after offset and linear drift removal. REF. 2–REF. 1: −234.9 mHz s^{-1}; silicon–REF. 1: −4.7 mHz s^{-1}; silicon–REF. 2: 230.2 mHz s^{-1}.

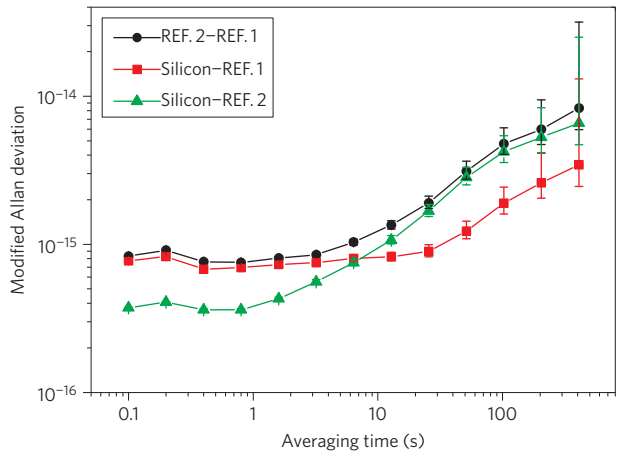

Figure 4 | Modified Allan deviation of the fractional frequency instability for the corresponding beat signals shown in Fig. 3.

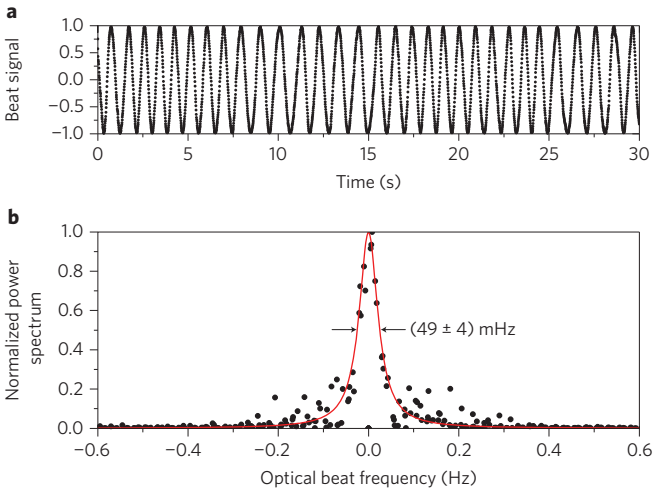

Figure 5 | Optical heterodyne beat between the silicon cavity system and REF. 2. a, Beat signal mixed down close to d.c. and recorded with a digital oscilloscope. **b**, Normalized fast Fourier transform of the beat signal recorded with a HP 3561A FFT analyser (37.5 mHz resolution bandwidth, Hanning window). A Lorentzian fit is indicated by the red line. The combined result of five consecutive recordings of the beat signal (black dots) is displayed here, demonstrating the robustness of this record-setting linewidth.

Figure 3 documents a typical 10 min trace of the beat signals between the three lasers under comparison after removal of the linear drift. The best long-term stability was observed for the beat between the silicon cavity-stabilized laser and REF. 1, with maximum frequency excursions of less than 3 Hz over the full time period. The two beat signals of silicon–REF. 2 and REF. 2–REF. 1 show that REF. 2 suffers from noise at a timescale of 10 s and beyond.

For detailed analysis of the frequency stability of the three systems, modified Allan deviations[39] were determined from the time records and are shown in Fig. 4 (error bars derived from χ^2 statistics[40,41]). The two laser beats involving REF. 1 are limited by flicker frequency noise to a level of mod $\sigma_y \approx 7 \times 10^{-16}$, which is consistent with the thermal noise floor expected for this reference laser. The flicker frequency noise of mod $\sigma_y \approx 3.3 \times 10^{-16}$ at 0.1–1 s averaging time for the beat between the silicon cavity-stabilized laser and REF. 2 can be attributed to a large extent to the thermal noise limit of REF. 2. Baseline fluctuations of the servo error signal by residual amplitude modulation were actively controlled to a level of $\sigma_y < 6 \times 10^{-17}$ for averaging times greater than 1 s (see Methods).

The narrowest optical linewidth was observed for the beat between the silicon laser and REF. 2. This signal was analysed by a digital oscilloscope (Fig. 5a) and a fast Fourier transform analyser (Fig. 5b). We obtained a typical full-width at half-maximum (FWHM) of 49(4) mHz, which is the narrowest spectrum of a beat between two lasers yet observed[15]. Considering that the silicon cavity-stabilized laser has the best stability of all three systems, it is a reasonable estimate that its linewidth is below 35 mHz. The optical coherence time is 10 s. Typically, 70% of the signal power is concentrated in the central carrier.

To evaluate the performance of each single laser, rigorous three-cornered hat analysis (including correlations between the three oscillators) was carried out according to ref. 42. To verify the reproducibility of the analysis the full data set was split into 130 data sets with a duration of 10 min each. For these data sets, three-cornered hat analysis was performed, including the effect of possible correlations between the laser systems[42]. The average instability of each of the three lasers is shown in Fig. 6 (error bars for the single oscillators represent the sample standard deviation of the mean values). The averaged Allan covariances are smaller by at least a factor of 10 compared to the individual Allan variances for all averaging times and therefore reflect the reliability of the three-cornered hat to the extent given by the error bars. The extracted covariances between the lasers are comparable in size and therefore do not indicate a pairwise correlation between the lasers or any common-mode behaviour.

At short averaging times the two reference lasers are limited to within a factor of two of their thermal noise floors of $\sim 6 \times 10^{-16}$ and $\sim 2 \times 10^{-16}$, respectively. The predicted thermal noise for the silicon cavity-stabilized laser of mod $\sigma_y \approx 5 \times 10^{-17}$ is indicated in the graph. Note that instabilities arising from flicker frequency noise in a modified Allan plot are reduced by ~18% in comparison to the commonly used standard Allan deviation. The stability of the laser locked to the silicon cavity clearly surpasses the performance of the two ULE-cavity-based reference lasers and consequently the silicon data contain the largest statistical uncertainty. The silicon cavity system reaches a residual fractional frequency instability of $\sim 1 \times 10^{-16}$ for averaging times of 0.1–1 s and remains at the low 10^{-16} level for averaging times up to 10 s, which is a timescale relevant for long-term stabilization to the strontium atomic frequency

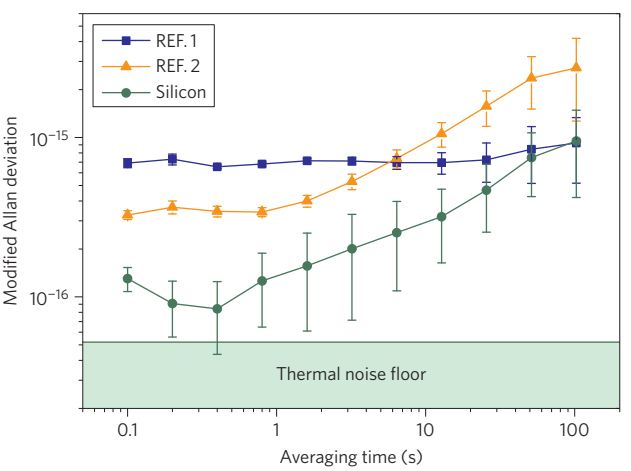

Figure 6 | Modified Allan deviation of each cavity-stabilized laser derived from a three-cornered hat analysis of the data in Fig. 3. The data show the average instability of 130 data sets with a duration of 10 min each. Error bars represent the standard deviation of the data averaged for each point. The predicted thermal noise floor of mod $\sigma_y \approx 5 \times 10^{-17}$ for the silicon cavity system is indicated by the shaded area.

standards[43] available at both JILA and PTB. The long-term performance was analysed in a transfer beat[44] against a hydrogen maser over a duration of 2 days, resulting in a linear frequency drift as low as 0.2 mHz s^{-1}. The single-day frequency variation was limited to below 19 Hz. These values are competitive with the most advanced cryogenic optical resonators[19,45].

The instability of the silicon cavity system at short timescales (below 0.5 s) was limited by the measured vibration noise floor and RAM. This level of performance represents the best fractional frequency stability to date for any oscillator—optical or microwave—for averaging times between 0.1 and 10 s. Such a stable cavity will have a direct impact on optical atomic clocks and will also have important implications for quantum metrology and precision measurement science in general.

Discussion

Our first investigations of silicon as a material for an optical reference cavity with ultralow thermal noise have already demonstrated performances that surpass any previously reported optical cavities. At this early stage, a number of technical challenges are yet to be mastered to reach the predicted thermal noise floor of mod $\sigma_y \approx 5 \times 10^{-17}$ and to further lower this limit. RAM errors in cavity servos can be suppressed to the required level by active feedback. However, for short timescales, the vibration noise of the cryostat should be further reduced. The mechanism that limits the instability to $\sim 1 \times 10^{-16}$ for averaging times of 1–100 s needs further investigation based on a direct comparison with a second silicon cavity-stabilized laser we are currently developing.

Material creep is not expected from a single-crystal cavity, so the cavity will also serve as an excellent long-term stable frequency reference, and is currently competitive with the stability of a hydrogen maser at timescales up to 1,000 s. The long-term stability for averaging times of a few days is currently being recorded in an extensive measurement investigation. The weekly refills of the cryostat have not shown any measurable effect on the laser performance and the laser has remained locked to the cavity over several months. In combination with an optical frequency comb, which allows the stability of the silicon system to be transferred to any wavelengths within the comb spectral coverage[44,46], the infrared ultra-stable laser will provide a powerful tool for high-resolution spectroscopy and optical clocks. With clock instabilities of $1 \times 10^{-16}/\sqrt{(\tau)}$ (τ in seconds), which will be possible with such a laser as the local oscillator, the observation times τ needed to resolve frequency shifts at a level of 10^{-17} would be at the 100 s level[43].

Finally, we note that the thermal noise limit of an optical cavity based on single-crystal silicon is currently set by the optical coating. We plan to investigate different approaches to push down this limit. Possible candidates for the next generation of optical coatings are microstructured gratings[47] or mirrors based on groups III and V such as gallium arsenide[48]. With these materials, an instability approaching 10^{-17}, and below, could be within reach.

Methods

We used two different commercially available finite-element simulation software packages for a rigorous simulation of the silicon cavity support structure, taking into account the full elasticity tensor of silicon. The two simulations results agree well within the tolerance error for machining. Three different mesh sizes (20 mm, 9 mm and 6 mm) were used and gave essentially the same simulation results. More information about simulations can be found in ref. 49. We found that for the silicon cavity, the horizontally supported (notched) cavity shows a factor of 3 worse vibration sensitivity than the vertical cavity geometry for a given tolerance of the mounting size and position.

FEM simulations were used to optimize the cavity mounting for REF. 1 for rigidity and small vibration sensitivity. Similar to the design in ref. 30, the cavity was supported at four points near the horizontal symmetry plane. The vibration sensitivity was verified as $<3 \times 10^{-10}/g$ in all three directions. The support geometry for the cavity of REF. 2 is similar to that in ref. 31. The spacer is a horizontally mounted cylinder. Support shelves extend the entire length of the spacer with four support points defined by small Teflon cylinders. The exact positions of the cylinders and the geometry of the support shelves were chosen by simulation to provide immunity to accelerations, and we verified that in all directions the vibration sensitivity was $<5 \times 10^{-10}/g$.

To apply phase-modulation sidebands for the PDH locking scheme, both the silicon system and REF. 2 used electrooptic modulators (EOMs) based on fibre-coupled $LiNbO_3$ waveguides. These modulators have the advantage that they require less than 1 V modulation voltage for an ~1 rad optical phase shift and also have a highly defined interaction region within the crystal, making them less susceptible to problems arising from crystal inhomogeneity or anisotropy of the applied field. However, it is difficult to ensure that the crystal extraordinary axis is aligned with the in-fibre light polarization, creating a polarization rotation effect at the drive frequency. We observe this effect as RAM at the radiofrequency drive frequency after a polarization analyser, and actively cancel it by applying a d.c. field to the crystal in addition to the radiofrequency drive[50]. This method of cancelling the residual polarization rotation is also effective at removing additional RAM due to intramodulator and intrafibre parasitic etalons, and the crystal piezoelectric response, resulting in a near-ideal fibre-coupled, broadband and low-voltage EOM. However, as with conventional modulators based on bulk crystals, etalons present in the optical system beyond the detection system can still introduce additional, uncancelled RAM. The active servo is beneficial at all timescales, and at 10 s and beyond lowers the RAM-induced frequency offset drift by more than an order of magnitude.

Received 10 February 2012; accepted 31 July 2012; published online 9 September 2012

References

1. Chou, C. W., Hume, D. B., Koelemeij, J. C. J., Wineland, D. J. & Rosenband, T. Frequency comparison of two high-accuracy Al^+ optical clocks. *Phys. Rev. Lett.* **104,** 070802 (2010).
2. Ludlow, A. D. *et al.* Sr lattice clock at 1×10^{-16} fractional uncertainty by remote optical evaluation with a Ca clock. *Science* **319,** 1805–1808 (2008).
3. Tamm, C., Weyers, S., Lipphardt, B. & Peik, E. Stray-field induced quadrupole shift and absolute frequency of the 688 THz $^{171}Yb^+$ single-ion optical frequency standard. *Phys. Rev. A* **80,** 043403 (2009).
4. Harry, G. M. *et al.* Thermal noise from optical coatings in gravitational wave detectors. *Appl. Opt.* **45,** 1569–1574 (2006).
5. Abbott, B. P. *et al.* LIGO: the laser interferometer gravitational-wave observatory. *Rep. Prog. Phys.* **72,** 076901 (2009).
6. Birnbaum, K. M. *et al.* Photon blockade in an optical cavity with one trapped atom. *Nature* **436,** 87–90 (2005).
7. Marshall, W., Simon, C., Penrose, R. & Bouwmeester, D. Towards quantum superpositions of a mirror. *Phys. Rev. Lett.* **91,** 130401 (2003).
8. Abbott, B. *et al.* Observation of a kilogram-scale oscillator near its quantum ground state. *New J. Phys.* **11,** 073032 (2009).
9. Eisele, C., Nevsky, A. Y. & Schiller, S. Laboratory test of the isotropy of light propagation at the 10^{-17} level. *Phys. Rev. Lett.* **103,** 090401 (2009).
10. Numata, K., Kemery, A. & Camp, J. Thermal-noise limit in the frequency stabilization of lasers with rigid cavities. *Phys. Rev. Lett.* **93,** 250602 (2004).
11. Notcutt, M. *et al.* Contribution of thermal noise to frequency stability of rigid optical cavity via Hertz-linewidth lasers. *Phys. Rev. A* **73,** 031804 (2006).
12. Kessler, T., Legero, T. & Sterr, U. Thermal noise in optical cavities revisited. *J. Opt. Soc. Am. B* **29,** 178–184 (2012).
13. Ludlow, A. D. *et al.* Compact, thermal-noise-limited optical cavity for diode laser stabilization at 1×10^{-15}. *Opt. Lett.* **32,** 641–643 (2007).
14. Young, B. C., Cruz, F. C., Itano, W. M. & Bergquist, J. C. Visible lasers with subhertz linewidths. *Phys. Rev. Lett.* **82,** 3799–3802 (1999).
15. Jiang, Y. Y. *et al.* Making optical atomic clocks more stable with 10^{-16} level laser stabilization.*Nature Photon.* **5,** 158–161 (2011).
16. Kimble, H. J., Lev, B. L. & Ye, J. Optical interferometers with reduced sensitivity to thermal noise. *Phys. Rev. Lett.* **101,** 260602 (2008).
17. Millo, J. *et al.* Ultrastable lasers based on vibration insensitive cavities. *Phys. Rev. A* **79,** 053829 (2009).
18. Legero, T., Kessler, T. & Sterr, U. Tuning the thermal expansion properties of optical reference cavities with fused silica mirrors. *J. Opt. Soc. Am. B* **27,** 914–919 (2010).
19. Storz, R., Braxmaier, C., Jäck, K., Pradl, O. & Schiller, S. Ultrahigh long-term dimensional stability of a sapphire cryogenic optical resonator. *Opt. Lett.* **23,** 1031–1033 (1998).
20. Seel, S., Storz, R., Ruoso, G., Mlynek, J. & Schiller, S. Cryogenic optical resonators: a new tool for laser frequency stabilization at the 1 Hz level. *Phys. Rev. Lett.* **78,** 4741–4744 (1997).
21. Nietzsche, S. *et al.* Cryogenic Q-factor measurement of optical substrates for optimization of gravitational wave detectors. *Supercond. Sci. Technol.* **19,** S293–S296 (2006).
22. Richard, J.-P. & Hamilton, J. J. Cryogenic monocrystalline silicon Fabry–Pérot cavity for the stabilization of laser frequency. *Rev. Sci. Instrum.* **62,** 2375–2378 (1991).
23. Schnabel, R. *et al.* Building blocks for future detectors: silicon test masses and 1550 nm laser light. *J. Phys. Conf. Ser.* **228,** 012029 (2010).

24. Petersen, K. E. Silicon as a mechanical material. *Proc. IEEE* **70,** 420–457 (1982).
25. Glassbrenner, C. J. & Slack, G. A. Thermal conductivity of silicon and germanium from 3 °K to the melting point. *Phys. Rev.* **134,** A1058–A1069 (1964).
26. Brantley, W. A. Calculated elastic constants for stress problems associated with semiconductor devices. *J. Appl. Phys.* **44,** 534–535 (1973).
27. Nawrodt, R. *et al.* A new apparatus for mechanical *Q*-factor measurements between 5 and 300 K. *Cryogenics* **46,** 718–723 (2006).
28. Harry, G. M. *et al.* Thermal noise in interferometric gravitational wave detectors due to dielectric optical coatings. *Class. Quantum Grav.* **19,** 897–917 (2002).
29. Notcutt, M., Ma, L.-S., Ye, J. & Hall, J. L. Simple and compact 1-Hz laser system via an improved mounting configuration of a reference cavity. *Opt. Lett.* **30,** 1815–1817 (2005).
30. Nazarova, T., Riehle, F. & Sterr, U. Vibration-insensitive reference cavity for an ultra-narrow-linewidth laser. *Appl. Phys. B* **83,** 531–536 (2006).
31. Webster, S. A., Oxborrow, M. & Gill, P. Vibration insensitive optical cavity. *Phys. Rev. A* **75,** 011801(R) (2007).
32. Drever, R. W. P. *et al.* Laser phase and frequency stabilization using an optical resonator. *Appl. Phys. B* **31,** 97–105 (1983).
33. Glazov, V. & Pashinkin, A. The thermophysical properties (heat capacity and thermal expansion) of single-crystal silicon. *High Temperature* **39,** 443–449 (2001).
34. Webster, S. & Gill, P. Force-insensitive optical cavity. *Opt. Lett.* **36,** 3572–3574 (2011).
35. Gray, J. E. & Allan, D. W. in *Proc. 28th Frequency Control Symposium* 243–246 (1974).
36. Ma, L.-S., Jungner, P., Ye, J. & Hall, J. L. Delivering the same optical frequency at two places: accurate cancellation of phase noise introduced by optical fiber or other time-varying path. *Opt. Lett.* **19,** 1777–1779 (1994).
37. Rubiola, E. On the measurement of frequency and of its sample variance with high-resolution counters. *Rev. Sci. Instrum.* **76,** 054703 (2005).
38. Dawkins, S. T., McFerran, J. J. & Luiten, A. N. Considerations on the measurement of the stability of oscillators with frequency counters. *IEEE Trans. Ultr. Ferr. Freq. Contr.* **54,** 918–925 (2007).
39. Allan, D. W. & Barnes, J. in *Proceedings of the 35th Annual Frequency Control Symposium*, 470–475 (Electronic Industries Association, 1981).
40. Greenhall, C. & Riley, W. in *Proc. 2003 PTTI Meeting* 267–280 (2003).
41. Riley, W. & Greenhall, C. Power law noise identification using the lag 1 autocorrelation. *IEEE Trans. Instrum. Meas.* **2004,** 576–580 (2004).
42. Premoli, A. & Tavella, P. A revisited three-cornered hat method for estimating frequency standard instability. *IEEE Trans. Instrum. Meas.* **42,** 7–13 (1993).
43. Swallows, M. D. *et al.* Suppression of collisional shifts in a strongly interacting lattice clock. *Science* **331,** 1043–1046 (2011).
44. Telle, H. R., Lipphardt, B. & Stenger, J. Kerr-lens mode-locked lasers as transfer oscillators for optical frequency measurements. *Appl. Phys. B* **74,** 1–6 (2002).
45. Hartnett, J. G., Nand, N. R. & Lu, C. Ultra-low-phase-noise cryocooled microwave dielectric-sapphire-resonator oscillators. *Appl. Phys. Lett.* **100,** 183501 (2012).
46. Schibli, T. R. *et al.* Optical frequency comb with submillihertz linewidth and more than 10 W average power. *Nature Photon.* **2,** 355–358 (2008).
47. Brückner, F. *et al.* Realization of a monolithic high-reflectivity cavity mirror from a single silicon crystal. *Phys. Rev. Lett.* **104,** 163903 (2010).
48. Cole, G. D., Gröblacher, S., Gugler, K., Gigan, S. & Aspelmeyer, M. Monocrystalline $Al_xGa_{1-x}As$ heterostructures for high-reflectivity high-*Q* micromechanical resonators in the megahertz regime. *Appl. Phys. Lett.* **92,** 261108 (2008).
49. Chen, L. *et al.* Vibration-induced elastic deformation of Fabry–Pérot cavities. *Phys. Rev. A* **74,** 053801 (2006).
50. Wong, N. C. & Hall, J. L. Servo control of amplitude modulation in frequency-modulation spectroscopy: demonstration of shot-noise-limited detection. *J. Opt. Soc. Am. B* **2,** 1527–1533 (1985).

Acknowledgements

This silicon cavity work was supported and developed jointly by the Centre for Quantum Engineering and Space-Time Research (QUEST), the Physikalisch-Technische Bundesanstalt (PTB), the JILA Physics Frontier Center (NSF) and the National Institute of Standards and Technology (NIST). The authors thank R. Lalezari of ATF for the coating of the silicon mirrors and Y. Lin of JILA for the initial finesse measurements. The authors also thank M. Notcutt and R. Fox for technical assistance with the construction of the second reference cavity. U. Kuetgens and D. Schulze are thanked for X-ray orientation of the spacer and mirrors, and G. Grosche for technical assistance with fibre noise cancellation. J. Ye thanks the Alexander von Humboldt Foundation for support.

Author contributions

U.S., L.C., F.R. and J.Y. designed the silicon cavity. T.K., C.H., M.J.M., T.L., U.S., J.Y. and F.R. devised the measurements. T.K., C.H., M.J.M. and T.L. performed the experiments. T.K., C.H., M.J.M., T.L. and C.G. analysed and discussed the data. T.K., C.H., M.J.M., T.L., J.Y., U.S. and F.R. wrote the manuscript.

Additional information

Reprints and permission information is available online at http://www.nature.com/reprints. Correspondence and requests for materials should be addressed to F.R. and J.Y.

Competing financial interests

The authors declare no competing financial interests.